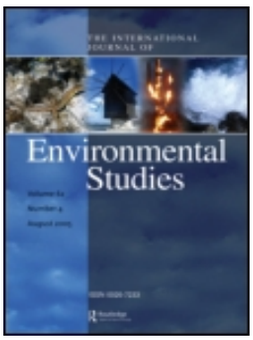

International Journal of Environmental Studies

ISSN: 0020-7233 (Print) 1029-0400 (Online) Journal homepage: https://www.tandfonline.com/loi/genv20

Lake water body mapping with multiresolution based image analysis from medium-resolution satellite imagery

Y. O. Ouma & R. Tateishi

To cite this article: Y. O. Ouma & R. Tateishi (2007) Lake water body mapping with multiresolution based image analysis from medium-resolution satellite imagery, International Journal of Environmental Studies, 64:3, 357-379, DOI: 10.1080/00207230500196856

To link to this article: https://doi.org/10.1080/00207230500196856

Published online: 14 Jun 2007.

International Journal of Environmental Studies,
Vol. 64, No. 3, June 2007, 357–379

Lake water body mapping with multiresolution based image analysis from medium-resolution satellite imagery

Y. O. OUMA* AND R. TATEISHI

Center for Environmental Remote Sensing, Chiba University, 1-33 YayoiInage-ku, Chiba, 263-8522, Japan

(Received 12 May 2005)

Shoreline mapping and shoreline change detection are critical for safe navigation, coastal resource management, coastal environmental protection and sustainable coastal development and planning. The main difficulty of traditional shoreline mapping from remote sensing classification is the lack of adequate tools to characterize and combine texture and spectral information effectively. This paper introduces a method for unsupervised lake shoreline delineation through combination of scene texture and spectral characteristics. The framework is based on multiresolution image segmentation via multispectral anisotropic diffusion neural network, in combination with texture derived from 2D-wavelet transform algorithm. We illustrate the application of this algorithm by extracting water body pixels from Landsat ETM+, TM and MSS for case study of Lake Nakuru in Kenya. The results are very superior compared to the conventional methods (NDWI) and indicate that the lake has reduced by 18.8% between 1976–2001.

Keywords: Geofeature discrimination; Lake water body/shoreline; Wavelet transforms; Anisotropic diffusion; Texture-based segmentation; Neural networks

1. Introduction

The accurate detection of change of water bodies and their catchments, in terms of distribution and variation, from remotely sensed imagery is important for the evaluation and monitoring of those resources. Due to the vast spread of water bodies, e.g. lakes and the inaccessibility of some of them, this information is always difficult to acquire. The process of assessment is associated with problems such as land–water interfaces, organic and inorganic constituents in water, resolution constraints and spectral similarity with clouds/shadows and western facing mountains sides. It is recognized that differences and similarities in measurement scales and feature distributions from multisource spatial data continue to impede analysis, in large scale hydrological modeling using remote sensing data.

Lake Nakuru in Kenya has shown uncharacteristic signs of change over the past decade – drying out each year (fluctuating in size); growing vast blooms of toxic algae; and experiencing

*Corresponding author. Email: yashon@graduate.chiba-u.jp

International Journal of Environmental Studies
ISSN 0020-7233 print: ISSN 1029-0400 online © 2007 Taylor & Francis Group
http://www.tandf.co.uk/journals
DOI: 10.1080/00207230500196856

Published online 14 Jun 2007

die-offs of large numbers of fish, waterfowl, waterbucks, and the park's most famous flamingoes: all likely victims of toxins in the lake. These changes result from increased population numbers, expanded settlements, growing small-scale farming and the discharge of pollutaants from a significant industrial sector; as well as vast modifications of landscape (e.g. deforestation and erosion) throughout the Lake Nakuru catchment basin. Mapping of the extent and variation of the lake is one of the measures of the impacts of the land use/land cover (LULC) changes as well as climatic conditions. This needs to be carried out regularly and accurately. The variation and extent mapping must be carried out in a multitemporal fashion to predict future scenarios and assist in continuous management.

The delineation and extraction of coastline and water bodies, e.g. rivers and lakes, is useful in different fields such as lake/coastline erosion monitoring, lake/coastal-zone management, watershed definition, flood prediction, and evaluation of water resources. This task is difficult for a huge region, such as an entire country or continent lakes/sea shorelines when using traditional ground survey techniques because water bodies can be fast moving as in floods, tides, and storm surges or may be inaccessible. In addition, automatic and replicable techniques are required to update coastline maps, evaluate the spatial and temporal evolution of alterations due to natural and anthropic events, and extract the waterline for vast regions. Following the increase in the availability of satellite images, the development of tools for geographic data analysis (GIS platforms) and image processing techniques, numerous research studies have been carried out to extract and delineate water bodies from these images. The extraction of features from satellite images overcomes the problem of matching available coastline data sets with the studied image dataset. In fact, owing to projection system biases, the matching of a shoreline coming from a different data set together with the available images may be a tedious if not impossible task.

Different algorithms supervised and unsupervised (e.g. ISO-DATA, principal components analysis [PCA], Tasseled Cap, normalized difference water index [NDWI]) have been implemented in the recent years to extract different water bodies: rivers, lakes and seas. In recent years, satellite remote sensing data has been used in automatic or semi-automatic shoreline extraction and mapping. Braud and Feng [1] evaluated threshold level slicing and multispectral image classification techniques for detection and delineation of the Louisiana shoreline from 30 m resolution Landsat Thematic Mapper (TM) imagery. They found that thresholding TM Band 5 was the most reliable methodology. Jupp *et al*. [2] analyzed the histogram of Landsat TM band 7 and segmented water pixels by thresholding. Moller-Jensen [3] did the thresholding in TM bands 4 and 5 and then recognized water pixels using experience-based rules. McFeeters [4] detected water bodies by thresholding the ratio of TM bands 3 and 4. Tasseled Cap Transformation, based on the statistical information of the various bands, has been used to calculate the Index of Wetness. Traditional methods, e.g. supervised maximum-likelihood, have also been used in the extraction of water bodies.

These approaches are highly dependent on: (1) human expert reliance; and (2) accurate radiometric and geometric correction for change derivation. There is a need for the development of automatic analysis tools that could be cost-effective in long-term and minimize these requirements.

1.1. Approach for automated lake shoreline detection

Figures 1(a) and (b) show the representation of the lake with the near-infrared (NIR) bands in Landsat ETM+ (2001) and Landsat MSS (1976). Evident are other near-by features (shown with arrows) that have the same reflectance as the lake e.g. sewer-plants in the ETM+ image,

(a)

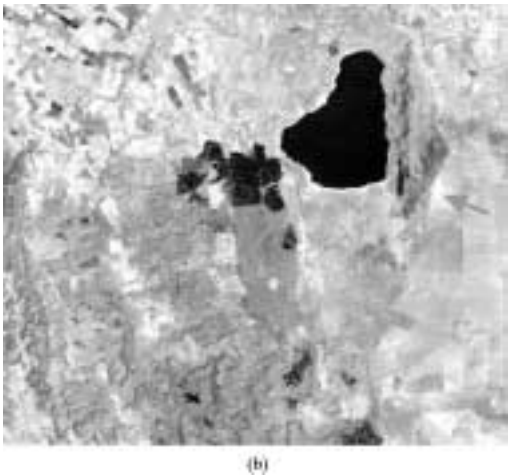

(b)

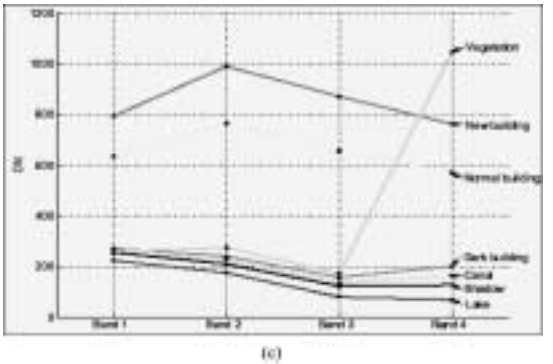

(c)

Figure 1. (a) 2001-Landsat ETM+ NIR band (4); (b) 1976-Landsat MSS NIR band (6). The arrows point at the similarly reflecting regions with the lake; (c) example spectral overlap problem in detecting water bodies from ETM+ visible and NIR bands.

water marshes, shadows on the hilly bounded side of the lake and water ponds in the MSS image. This poses spectral confusion (figure 1(c)) especially if conventional methods are used to extract features of interest (FOI), which have typically used iterative thresholding to reach the desired solution.

In recent years, there has been mention of the utility of wavelet transforms [5] and neural networks ([6], [7], [8]) for the extraction of specific features from remotely sensed data. Results have been reported to be more accurate and automated. The application of these techniques in water body extraction has received little or no research attention at all, yet water resource monitoring is a global priority.

While wavelet analysis is gaining popularity as a framework for handling multiresolution data suitable for extracting information from noisy signals and for modeling non-stationary phenomena, the use of artificial neural networks in this field is highly adaptive, needs no *a priori* knowledge and can be computed parallel-wise. Wavelets analysis is suitable for extracting scene texture. Integration of texture and spectral information is important for enhancing geofeature recognition in satellite imagery. One way of doing this is via anisotropic diffusion process that combines spectral and spatial information. Anisotropic diffusion (AD) allows for intra-region smoothing without inter-region smoothing; hence it is suitable for simultaneous enhancement and segmentation of remote sensing data. Anisotropic diffusion method is attractive due to its preservation of edge localization and ability to control feature scale [9]. Combining wavelets and AD in a neural network scheme in analyzing spectral and texture information is suggested in this research. We apply this to the discrimination of lake water body as a FOI, based on automatic resolution thresholding.

In this paper, we first pose the following questions: what is FOI and why is feature selection important? Within the scope of remote sensing and GIS applications, a feature is a variable or attribute. The objective of detection and extraction of FOI is to eliminate noisy and irrelevant features within the same scene and discover the most important/relevant features (FOI). To define FOI, we proposed the use of anisotropic diffusion as an image enhancement method. This is a non-linear process, which removes noise and irrelevant details while preserving the edges, i.e. it extracts the essential visual information. We give a theoretical review of the techniques, the implementation strategy and then present the results of our experiments. The framework is used for automated extraction, visualization and change detection of the lake water body from multiresolution, multispectral and multitemporal (MMM)-Landsat imagery dated 1976, 1986 and 2001, respectively. The objectives of this study are: (1) to implement automated recognition and visualization strategy as a means of delineating varying sized, shaped and spatially distributed feature, in this case lake water body. (2) To minimize the sensitivity of multitemporal feature extraction and change visualization to radiometric and geometric registration factors by using multiscale image analysis techniques.

Our approach is to combine spectral and spatial information for the images using wavelets and anisotropic diffusion segmentation techniques. The proposed approach integrates spectral analysis with texture and morphology in a scale-space fashion to analyze homogeneous regions in multitemporal satellite imagery. The new method is compared with the simple NDWI and digitized aerial photo products to illustrates its' advantage(s) with respect to FOI isolation.

The scope of the current research is not to determine/quantify the change in the Lake Nakuru water levels, but test the proposed methodology as an automatic lake water body delineation approach and extend it slightly to determine the shoreline and surface area of the lake, within a mixed scene as seen in the test images. Next and most important is that the proposed multiscale image analysis has the advantage of analyzing the features within a

scene such that as the resolution changes from fine to coarse, larger specific or homogeneous landscape features are magnified. Our approach represses the smaller features that cannot be represented as continuous and homogenous features at this spatial resolution. In other words it may be only significant to determine or isolate a lake from 120 m spatial resolution and not 1 m resolution. To isolate the lake from a nearby pond, varied spatial resolutions have to be applied. This will ensure reduced processing time in accuracy assessment with respect to false alarm features detection as compared to the semi-automated conventional methods. This argument may be summarized in light of the recent and rapidly advancing scale-space theory for landscape analysis from satellite remote sensing.

2. Study site and experimental data

2.1. Study site

The test area is Lake Nakuru in Kenya. Lake Nakuru, located in the East African Rift valley, is protected by a surrounding National Park that covers 90 square miles. It is located between 0° 24′ 0″ S and 36° 5′ 0″ E (figure 2). The experimental data used in this study are summarized in table 1.

3. Multiresolution image analysis

3.1. FOI discrimination

In many real-world classification applications, a number of features are often computed to aid the supervised learning. Some of the candidate features, however, may be *irrelevant*, in

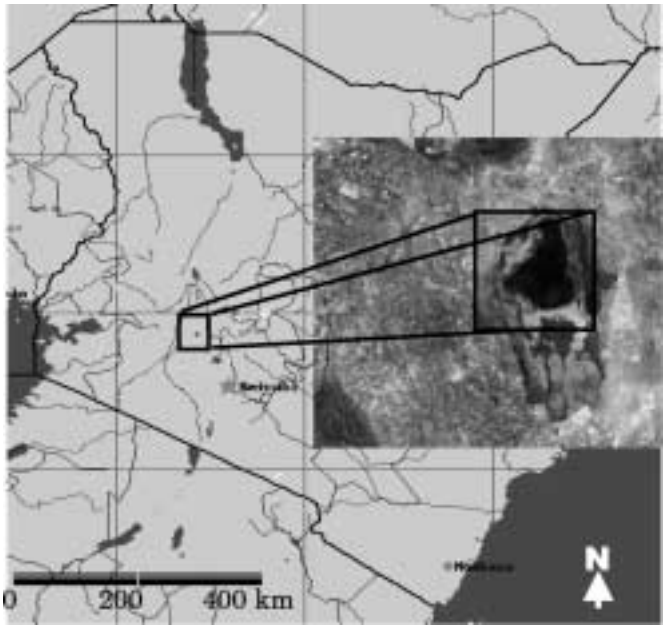

Figure 2. Map of Kenya and Lake Nakuru (inset ETM+ 432 false color composite imagery).

Table 1. Experimental data

Test site	Data	Size	Date of acquisition
Lake Nakuru, in Kenya	Landsat ETM+	1024 × 1024	3 April 2001
	Landsat TM	1024 × 1024	28 January 1986
	Landsat MSS	512 × 512	25 January 1976
	1:50,000 (TOPO)		1997 (partially revised)
	1:25,000 (VEGETATION)		1976 (#)

that they may be adding noise to useful information, or *redundant* in the presence of other relevant features. This is inevitable when assessing remote sensing data. A feature selection algorithm addresses this problem by selecting a subset of features, which are directly relevant to the target concept. Eigenspace methods like the principal component analysis (PCA) can be used to transform the feature space to a set of independent and orthogonal axes and rank those axes by the extent of variation. This is one way to reduce the set of features with regard to the global data covariance. Fisher's linear discriminant analysis (LDA), on the other hand, finds the feature space mapping which maximizes the ratio of between-class to within-class variation jointly for each feature (dimension). PCA can be further applied to find a compact subspace to reduce the feature dimensionality. PCA and LDA do not result in the straightforward automated process.

Wavelets and other multiresolution techniques have been developed in recent years, and furnish a powerful representation of data. Scale-space theory was developed to find those operators on images that extract fundamental psycho-visual information such as shapes and boundaries. By means of multiresolution or multiscale analysis, an image can be decomposed into a set of images (or scales), each scale containing only structures of a given size and type with certain accuracy. This data representation, associated with noise modeling, has been applied to very different applications such as data filtering, deconvolution, compression, but hardly in environmental remote sensing data analysis.

The flood of remote sensing data and related GIS data offers new potential for challenges in the development and implementation for dealing explicitly with scale. As the various scale remote sensed data are used in land cover/land use and vegetation mapping [10], environmental modeling [11], biophysical and landscape processes [12] and natural social interaction [13] over the past 20 years, there are extensive literatures showing that models and measurements of many phenomena are scale-dependent. In other words the factor of scale and resolution is seen to play an increasing important role in the employment of remotely sensed imagery [14,15].

Developing automated methods for characterizing, analyzing and displaying various types of multiscale remotely sensed data is important for the following reasons: (1) spatial resolution is one of the fundamental considerations of the remotely sensed data quality. It is important because it defines the size of the smallest observable units that constitute the set of spectral measurements used in the study [16]. Each scale corresponds to the measurement level of geographic detail. (2) The spatial variation of remotely sensed image is a function of spatial resolution. Therefore it is important relate the spatial variation at one scale to that of another. This introduces an automated sense of searching the most optimal resolution for specific feature mapping instead of the conventional semi-automated thresholding.

3.2. Multiresolution analysis (MRA)

A function or signal can be viewed as being composed of a smooth background and fluctuations or details on top of it. The distinction between the smooth part and the details is determined by the resolution, that is, by the scale below which the details of a signal cannot be discerned. At a given resolution, a signal is approximated by ignoring all fluctuations below that scale. We can imagine progressively increasing the resolution; at each stage of the increase in resolution finer details are added to the coarser description, providing a successively better approximation to the signal. Eventually when the resolution goes to infinity, we recover the exact signal.

A series of nested subspaces V_j, which is spanned by the orthonormal basis $\phi_{j,k}(t)$, $k \in Z$, forms a multiresolution space. The subspace W_j, which is spanned by the orthonormal basis $\phi_{j,k}(t)$, $k \in Z$, is the complementary space of V_j is the subspace V_{j-1} (figure 3). With $V_{j-1} = V_j \oplus W_j$. The subspaces V_j and W_j are called the approximation (A) and detail (D) spaces respectively at resolution j. As the scales vary, different features are detected either wholly or in part i.e. at two or more levels. These informative levels may later be combined for accurate feature extraction.

3.3. Multiresolution wavelet decomposition for texture extraction

Mallatt [17] developed the theory for multiresolution signal decomposition using the orthonormal wavelet basis and proposed its extension to texture analysis. A wavelet is a waveform of effectively limited duration that has an average value of zero. So, wavelet analysis is carried out by breaking up a signal into shifted and scaled versions of the original (mother) wavelet. From this, we can define a continuous wavelet transform as the sum over all time of the signal multiplied by a scaled and shifted version of the wavelet function ψ:

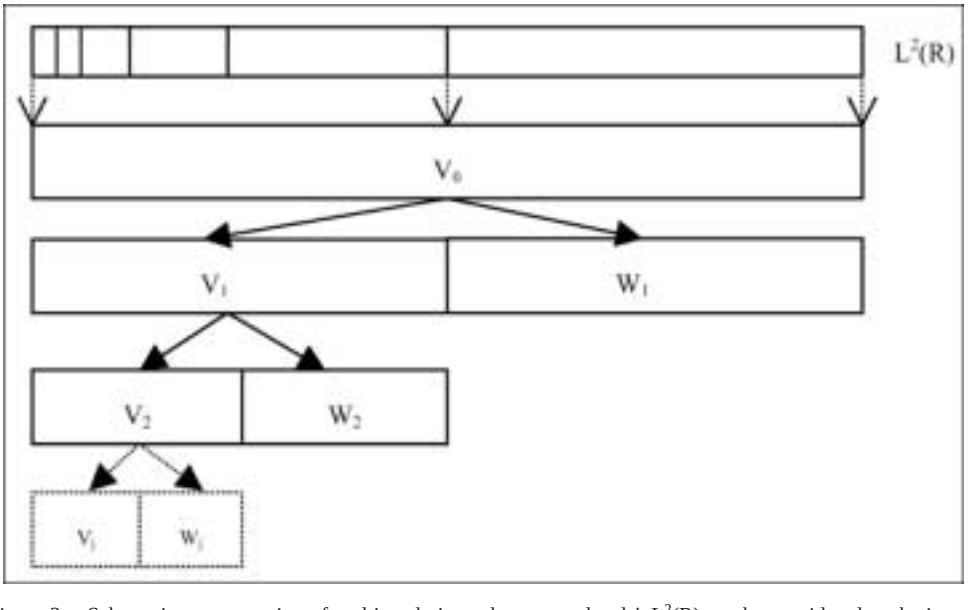

Figure 3. Schematic representation of multiresolution subspaces at level j. $L^2(R)$ can be considered as the image original image space defined in discrete subspaces and V_0 the input image, at level 0, of the multiscale analysis.

$$C(scale,\ position) = \int_{-\infty}^{\infty} f(t)\psi(scale,\ position) \tag{1}$$

Texture plays an important role in pattern recognition, image interpretation and segmentation in a variety of applications. Texture may be described as 'the visual impression of coarseness or smoothness caused by the variability or uniformity of image tone or color'. Lark [18] described a working definition of texture that includes two components: (1) the variability of DN values (regardless of spatial relations) and (2) the spatial dependence of this variability. Lark [18] concluded that 'two segments of an image may be regarded as having the same texture if they do not differ significantly with respect to: (a) the variance of their DN values; (b) the spatial dependence of this variability at a characteristics scale (or scales); (c) the directional dependence of this variability, and (d) any spatial periodicity of this variation.'

The multiresolution wavelet transform decomposes a signal into low frequency approximation and high frequency detail information at a coarser resolution. The resultant approximation is then decomposed into second level (coarser resolution) of approximation and detail, iteratively. The detail images are considered to be more relevant to the texture characteristics than the approximation sub-images. Figure 4 depicts a wavelet decomposition tree.

In satellite image analysis using 2D wavelet transform techniques, rows and columns of image pixels are considered signals. The approximation and details of a 2D-image *f(x,y)* at resolution 2^j can be defined by the coefficients computed by the following convolutions:

$$A^d \frac{j}{2} f = ((f(x,y) * \Phi\ \tfrac{j}{2}(-x)\Phi\ \tfrac{j}{2}(-y))(2^{-j}n, 2^{-j}m))_{(n,m)\varepsilon Z^2} \tag{2}$$

$$D^1 \frac{j}{2} f = ((f(x,y) * \Phi\ \tfrac{j}{2}(-x)\psi\ \tfrac{j}{2}(-y))(2^{-j}n, 2^{-j}m))_{(n,m)\varepsilon Z^2} \tag{3}$$

$$D^2 \frac{j}{2} f = ((f(x,y) * \psi\ \tfrac{j}{2}(-x)\Phi\ \tfrac{j}{2}(-y))(2^{-j}n, 2^{-j}m))_{(n,m)\varepsilon Z^2} \tag{4}$$

$$D^3 \frac{j}{2} f = ((f(x,y) * \psi\ \tfrac{j}{2}(-x)\psi\ \tfrac{j}{2}(-y))(2^{-j}n, 2^{-j}m))_{(n,m)\varepsilon Z^2} \tag{5}$$

where the integer j is a decomposition level, (m,n) are integers, $\Phi(x)$ is 1D-scaling function (low pass filter), and $\psi(x)$ is 1D-wavelet function (high pass filter). In general, $\Phi(x)$ is a smoothing function, which provides low frequency information, and $\psi(x)$ is a differencing function, which provides high frequency information [19]. Figure 5 shows how the original image $A^d \frac{j+1}{2} f$ is decomposed into $A^d \frac{j}{2} f$, $D^1 \frac{j}{2} f$, $D^2 \frac{j}{2} f$ and $D^3 \frac{j}{2} f$ sub-images. ($A^d \frac{j}{2} f$ = approximation sub-image, $D^1 \frac{j}{2} f$ = horizontal detail sub-image, $D^2 \frac{j}{2} f$ = vertical detail sub-image, $D^3 \frac{j}{2} f$ = diagonal detail sub-image, *Lo_F* = low-pass filter convolution, *Hi_F* = high-pass filter convolution, $2\downarrow$ = downsampling by factor of 2) [19,20].

Once the textures are detected at several scales, we must understand how to integrate this multiscale information for feature pattern recognition. One might be tempted to look for the 'best' scale where the textures are well discriminated from noises and feature textures. The

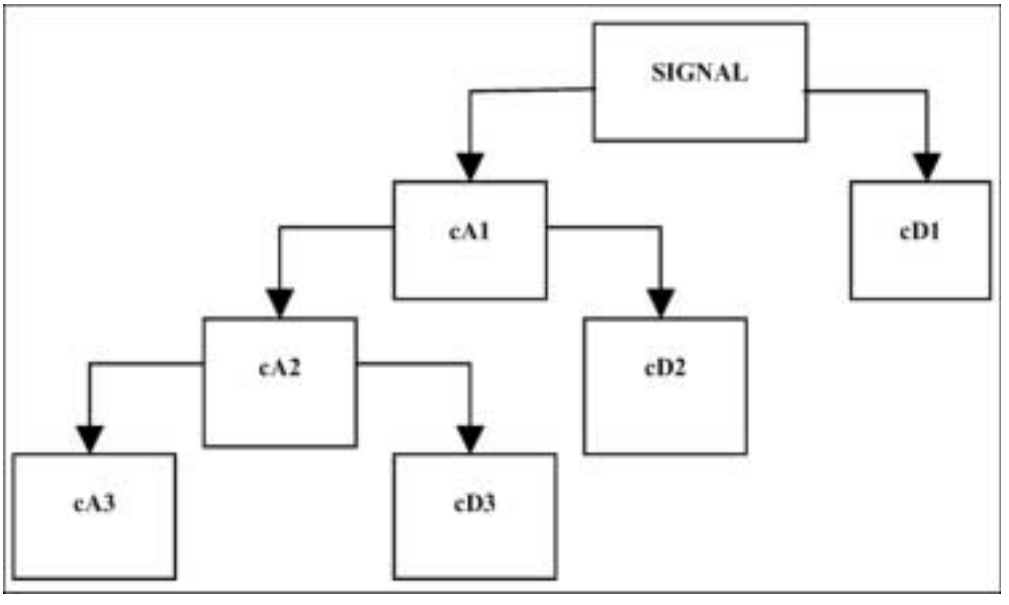

Figure 4. A signals decomposition tree, where *cAi* = approximation and *cDi* = details. Each detail level contains three subbands: vertical, horizontal and diagonal.

wavelet theory shows that much finer properties are derived by analyzing texture behaviours across scales. One way of analyzing multiscale texture in combination with spectral information is via anisotropic diffusion process (ADP).

3.4. Multispectral anisotropic diffusion

The idea behind the use of the diffusion equation in image processing arose from the use of the Gaussian filter in multi-scale image analysis. Convolving an image with a Gaussian filter K_σ:

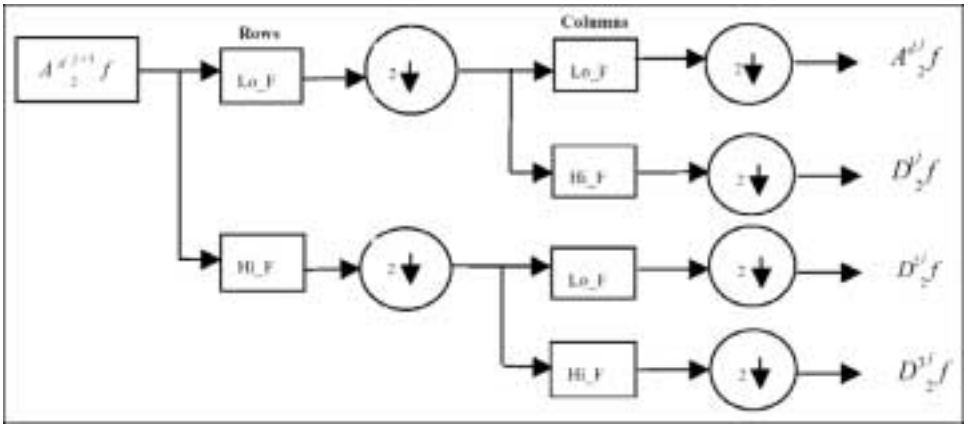

Figure 5. Multilevel wavelet decomposition algorithm representation. The results are texture maps and approximation image at each level of decomposition.

$$K_\sigma(x,y) = \frac{1}{2\pi\sigma^2}\exp\left(-\frac{|x|^2+|y|^2}{2\sigma^2}\right) \tag{6}$$

with standard deviation σ, is equivalent to the solution of the diffusion equation [21] in two dimensions:

$$\frac{\partial}{\partial t}I(x,y,t) = \nabla I(x,y,t) = \frac{\partial^2}{\partial x^2}I(x,y,t) + \frac{\partial^2}{\partial y^2}I(x,y,t) \tag{7}$$

where *I(x,y,t)* is the two-dimensional image *I(x,y)* at time $t = 0.5\sigma^2$, with initial conditions $I(x,y,0) = I_0(x,y)$, where I_0 is the original image. In general, this can be written as:

$$\frac{\partial}{\partial t}I(x,y,t) = \nabla\cdot(C(x,y,t)\nabla I(x,y,t)) \tag{8}$$

$$I(x,y,0) = I_0(x,y) \tag{9}$$

where *C(x,y,t)* is the diffusion conductance or diffusivity of the equation, ∇ is the gradient operator, and $\nabla\cdot$ is the divergence operator. If *c* is a constant, independent of *x*, *y*, or *t*, it leads to a linear diffusion equation, with a homogeneous diffusivity. In this case, all locations in the image, including the edges are smoothed equally. This is, of course, undesirable, and a simple improvement would be to change *c* with the location *x* and *y* in the image, thus converting the equation into a linear diffusion equation with non-homogeneous diffusivity. If the function *c* is image dependent, then the linear diffusion equation becomes a non-linear diffusion equation. By using a function *c* that was based on the derivative of the image at time *t*, they were able to control the diffusion near the edges in the image. Since then, several authors have enhanced this approach, and various options have been suggested for the diffusivity function, spatial discretization of the non-linear operator, and the numerical solution of the partial differential equation.

In their work, Perona and Malik [21,22], as several other authors, use the term 'anisotropic' to refer to the case where the diffusivity is a scalar function varying with the location. In the partial differential equation community, this case is referred to as non-homogeneous nonlinear isotropic diffusion. Non-homogeneous isotropic diffusion limits the smoothing of an image near pixels with a large gradient magnitude, which are essentially the edge pixels. As the diffusion near an edge is minimal, the noise reduction near the edge is also small. Accordingly, anisotropic diffusion was proposed to allow the diffusion to be different along different directions defined by the local geometry of the image.

The anisotropic form of the diffusion equation can be written as:

$$\frac{\partial}{\partial t}I(x,y,t) = \nabla\cdot(D(x,y,t)\nabla I(x,y,t)) \tag{10}$$

where $D(x, y, t)$ is a symmetric positive-definite diffusion tensor. This 2×2 matrix can be written in terms of its eigenvectors $\mathbf{v}_1$ and $\mathbf{v}_2$, and eigenvalues λ_1 and λ_2, as follows:

$$D = [\mathrm{v}_1 \quad \mathrm{v}_2]\begin{bmatrix}\lambda_1 & 0\\ 0 & \lambda_2\end{bmatrix}\begin{bmatrix}\mathrm{v}_1^{\mathrm{T}}\\ \mathrm{v}_2^{\mathrm{T}}\end{bmatrix} \tag{11}$$

By appropriately choosing the eigenvalues and eigenvectors, different diffusivity tensors can be obtained. In this paper, we focus on edge-enhancing diffusion, where the eigenvectors are defined as follows:

$$\mathrm{v}_1 \| \nabla I_\sigma \quad \text{and} \quad \mathrm{v}_2 \perp \nabla I_\sigma \tag{12}$$

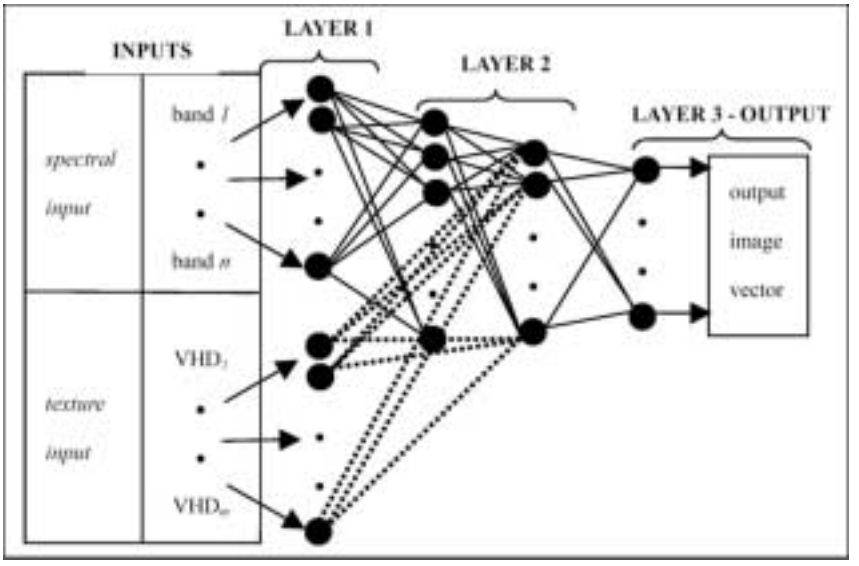

Figure 6. Anisotropic diffusion neural network (NN) concept. The NN consists of three layers: input, hidden and output. VHD_i are the vertical, horizontal and diagonal texture subbands from the wavelets transform process.

here, I_σ is the regularized (or smoothed) version of the image, that is, the image convolved with a Gaussian filter with standard deviation σ. Usually $\lambda_2 = 1$ to allow smoothing in the $\mathbf{v}_2$ direction. λ_1 can be chosen to be any of the diffusivity functions from the traditional non-homogeneous isotropic diffusion equation. This limits the diffusion in the direction of the gradient. The anisotropic diffusion method is more attractive due to its attractive preservation of edge localization [22] and the ability to control feature scale [23], hence its suitability as a discrimination procedure.

4. Recognition and visualization with proposed framework

4.1. Concept and hypothesis

The objective of the texture detection process is to detect sharp variations of an image *I(x,y)* in the direction of maximum change of the surface. Texture-based segmentation divides the image into 'homogenous' regions where local texture properties are approximately invariant. The goal is to find a minimum number of measurements that can discriminate textures perceived to be 'different'. The measurements should also remain approximately constant in a region where the texture is considered to be homogenous.

The orientation of texture elements and their frequency contents seem to be important clues for discrimination. This has motivated early researchers to study the repartition of texture energy in the Fourier domain. For segmentation purposes, it is, however, necessary to localize texture measurements over neighborhoods of varying sizes. For segmentation, the difficulty is to find an algorithm that aggregates the wavelet responses at all scales and orientations in order to find the boundaries of homogeneous textured regions. ADP is suggested for the aggregation of the wavelet transform coefficients, figure 6.

4.2. Experimental approach

The multiresolution decomposition provides users with possibility of a scale-invariant interpretation of the image. In wavelet transformation, different physical structures of the scene can be characterized at different resolutions based on the details of the image from coarse-to-fine. Coarse resolution provides the image 'context' that corresponds to the larger structure. This is useful as a pattern recognition strategy within the spectral image feature space.

The strategy used in this research to recognize the lake water body is called combined Wavelet-Anisotropic Diffusion. Figure 6 gives an overview of the combined scheme in neural network and figure 7 shows the entire research flow. The data processing steps included the following main tasks:

- Selection of appropriate band/data combination to extract spectral and textural information. Hence the principal components transform (PCT) band 1 (PC1) was used to extract texture information, as it is the albedo image (with the highest (98.41%) scene variance).
- Segmentation of the spectral band(s) with multiscale texture maps using the unsupervised anisotropic diffusion algorithm. The output of this stage is multiresolution image data that was used in the next step to extract the lake water body.

The unsupervised multilevel neural network (anisotropic diffusion neural network) used in this study modifies the pixel values of the input image by consecutive weighted averaging with neighboring pixels. It performs simultaneous modification of all input multispectral image at five levels of scale/resolution. This multilevel design process the spectral information of the image and textural details resulting from wavelet transformation simultaneously in a multiscale representation.

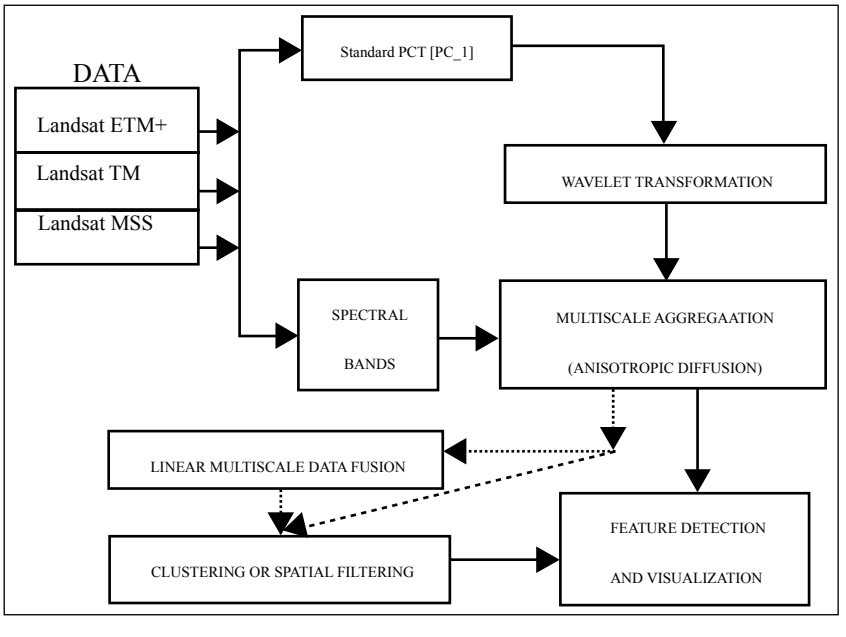

Figure 7. Experimental schema for feature detection and discrimination, with alternative processing paths.

In summary, we extract a window-size image from the input image. In the first phase, an extracted window-size image is decomposed into three sub-images using the texture transform. The decomposition is repeated until the minimal size of the sub-image has been exceeded. The results of this phase are texture images (maps) that contain a set of feature vectors. These feature vectors that correspond to different resolution of decomposed image are assumed to capture and characterize different scales of textures from the input image effectively. Anisotropic diffusion algorithm is then applied to combine texture and spectral feature vectors for aggregation, at different levels of scale in the next phase.

4.3. Multiscale texture data generation

Mallat's discrete 2D-wavelet transform algorithm was used to create multiscale texture maps from the first principal components transform (PC1) imagery of the test data sets. The transformation was carried at three scales for both data types. In wavelet transform, each scale has three detail images containing vertical, horizontal and diagonal information. Figures 9, 10 and 11 show the textural information that is extracted from the Landsat MSS, TM and ETM+ PC1 data, figure 8.

The vertical imagery contains image into information with spatial frequency energy oriented in the vertical direction (V), second detail image represents horizontal spatial frequency (H) while the third detail image contains the diagonal spatial energy information (D).

4.4. Spectral-texture aggregation

Multispectral anisotropic diffusion (MAD) neural network was used to segment the spectral Landsat -ETM+, -TM and -MSS images according to the texture maps. The algorithm does not perform image classification; therefore no training data is required. The input spectral data for this phase were the spectral bands of the ETM+ (bands 1,2,3,4,5,7), TM (bands 1,2,3,4,5,7) and MSS (1, 2,3,4). Using texture and spectral information, the amount of modification at given scales and locations was determined. Figure 12 shows the results of the levels 2 and 3 and their product.

Level 2 results (figure 12(a), (d) and (g)) and the products of level 2 and 3 (figure 12(c), (f) and (i)) were tested. Level 2 yielded superior results than level 3 and their product. The product image was tested since the aggregation process sometimes leads to loss of details as a result of smoothing at coarser resolutions. It is however advised that other combinations like summation of different levels may also be tested.

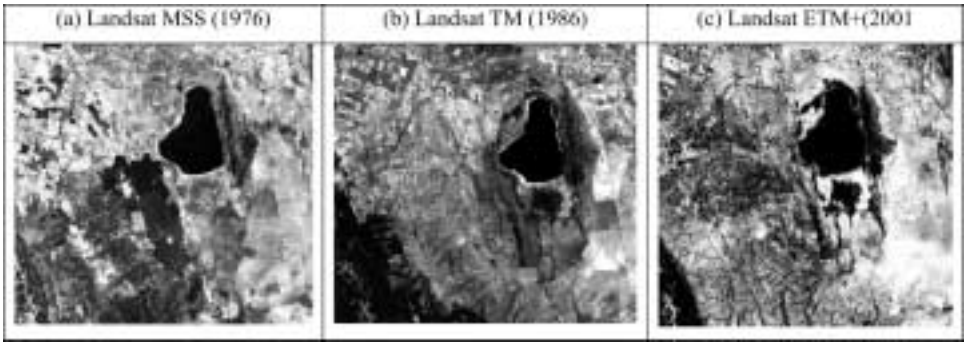

Figure 8. Input PC1 multitemporal images.

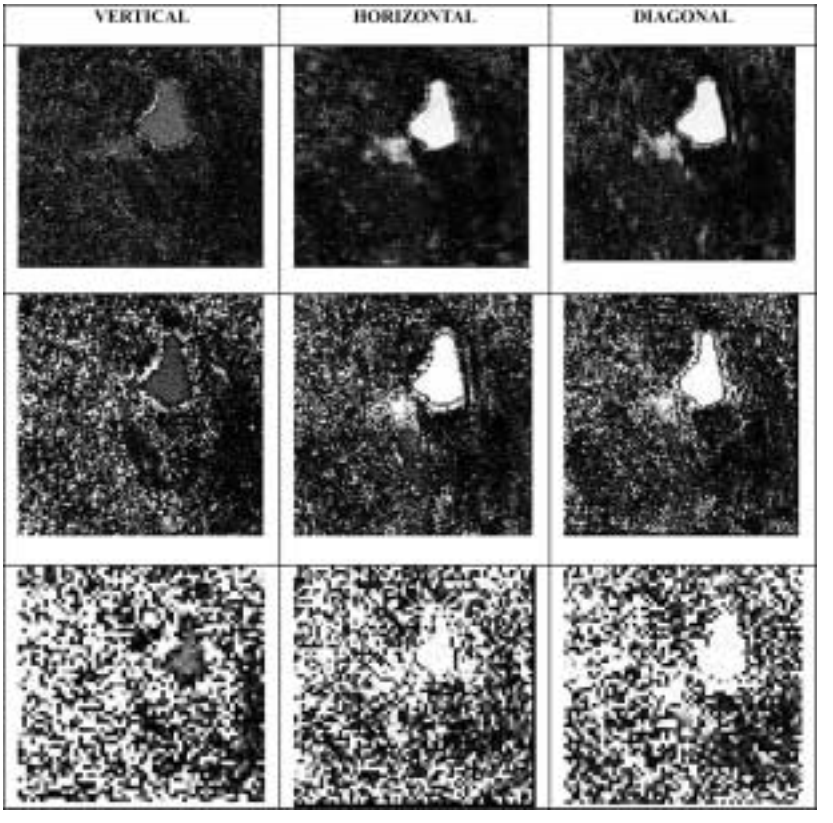

Figure 9. Landsat MSS three level decomposed sub-images: vertical (V), horizontal (H) and diagonal (D) subbands for levels 1, 2 and 3, respectively.

4.5. Image enhancements and morphological filtering

Image enhancement and morphological filtering were implemented in order to remove non-water and other sharp spikes that were considered as residuals to level 2 images and to finally define the lake with respect to size, shape and location. Mathematical morphology filtering is a non-linear method of processing digital images on the basis of shape. Its primary goal is the quantification of geometrical structures. Closing filters smooth the contours, fuse narrow breaks and long thin gulfs, eliminate small holes, and fill gaps in the contours of an image (figure 13(a)). The closing of an image is defined as the dilation of the image followed by subsequent erosion using the same structural element. Appropriate window setting eliminates the very small patches while maintaining the size of the predominant feature(s). Figure 13(b) presents the results of the enhancement and 7×7 morphological filtering respectively, smoothened image.

5. Discussion

5.1. Lake shoreline detection results analysis and comparison

As already stated, the scope of the current research is to determine the shoreline and estimate the area of lake water body accurately, while suppressing similarly reflecting bodies as seen

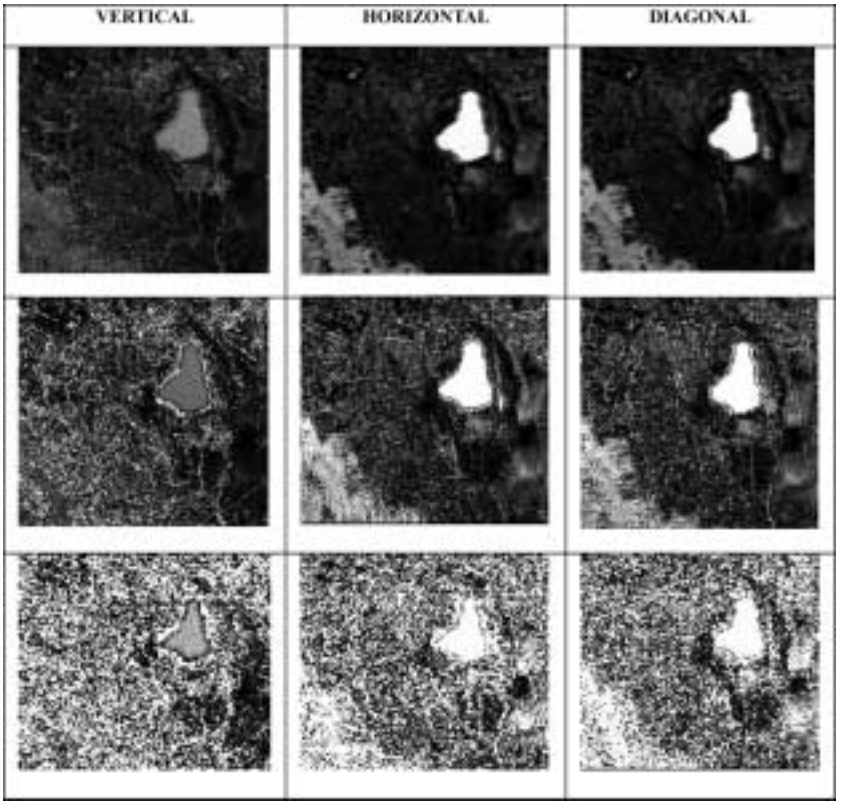

Figure 10. Landsat TM three level decomposed sub-images: V, H and D subbands for levels 1, 2 and 3.

in the test images. Lake Nakuru with a mean depth of 2.5 m and maximum depth of 4.5 m and varying surface areas of between 5–45 km^2 exhibits a highly fluctuating phenomenon. This in part affects the aquatic life of, for example flamingoes, and also economic activities like fishing and tourism. These fluctuations around and within the lake, are irregular and are induced both by climate and land use/land cover changes.

Figure 13(b) shows the results of the proposed approach. From water pixels counting, the results indicate that between 1976 and 1986, the lake shrank by about 7.2%, and 11.6% between 1986 and 2001. These changes were mostly in the western side of the lake, since a steep mountain bounds the eastern side. These changes translate into the surface area of Lake Nakuru being 41.10, 38.14 and 33.37 km^2, respectively, for the dates: 25 January 1976, 28 January 1986 and 3 April 2001.

To test the accuracy of the results, the available aerial photography derived topographic map was used for the 1976 scenario. In comparison to scanned and re-projected 1976 topographic map, figure 14, the accuracy of the delineated lake was (–2.7%) with respect to area estimate using the mean of planimetric area measurement. This is acceptable accuracy given that the lake fluctuates within the range of (10–90%) approximately.

The results were also compared using NDWI within three spectral domains (green) near-infrared (NIR) and short-wave infrared (SWIR). The first NDWI which is obtained using the function (Green - NIR)/(Green + NIR), is useful to demarcate the land–water boundary.

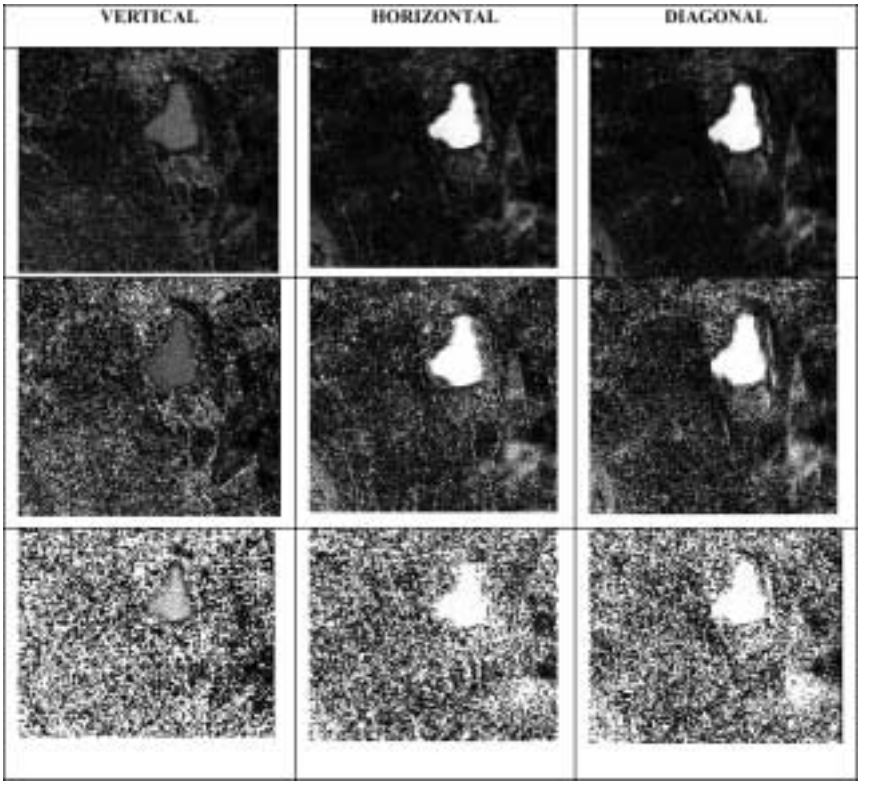

Figure 11. Landsat ETM+ three level decomposed sub-images: V, H and D sub-images for levels 1, 2 and 3.

Application of this technique for a multispectral satellite image results in positive values for water features and zero or negative values for soil and vegetation [4]. When the NDWI is applied using Band 2 (green) and Band 4 (NIR) data of the MSS, TM and ETM+ images of the lake region the results in figure 15(a–c) were obtained. Generally, in the case of ETM+ and MSS, lake water is not separable (distinct) from similarly reflecting spectral regions. However for TM, the results are good even though there persist some irrelevant or undesired features.

A second NDWI using (NIR - SWIR)/(NIR + SWIR) was computed. SWIR is band 5 in both ETM+ and TM. The results for the second NDWI are presented in figure 16(a) - ETM+ and figure 16(b) – TM. MSS does not have the SWIR band used in calculating the second NDWI. Comparing the results, the following observations were made: (1) NDWI retains many homogenous areas with similar spectral reflectance as the lake water; (2) the shoreline from NDWI results is fuzzy or noisy as compared to the results from our proposed approach; and (3) better results from NDWI can only be achieved via further manual (semi-automated) analysis. Clearly neither of the two NDWIs computed gave suitable results. From the above observations, we propose in future to utilize the NDWI as input band into our proposed method and not as a complete method in itself. Another important and advantageous observation is that the bands used for NDWI computation determine the end results especially is there if the dates of acquisition are different by months (three in our case). For example, for TM, the first NDWI presents better results than the second though there persists some confusion. This implies that NDWI is sensitive to multitemporal and radiometric feature

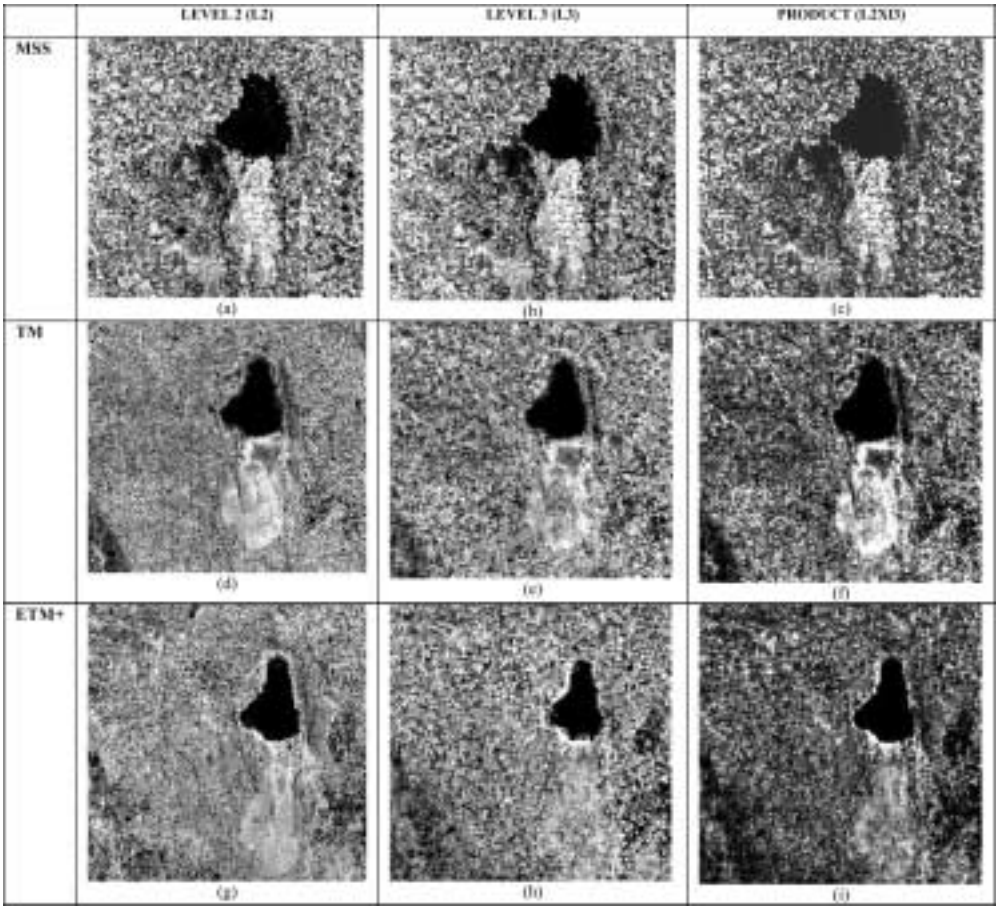

Figure 12. Selected second and third level textural-spectral segmentation results of MSS (a, b), TM (d, e) and ETM+ (g, h) imagery and their products (c), (f) and (i), respectively.

characteristics, suggesting a detailed and accurate pre-processing and manual trial and error approach, that even though is computationally cheap, may not be reproducible for other scenarios. Another problem within the scene is that the lake is very shallow (average 2.3 m deep). This is the same depth as sewerplants or even natural ponds around the lake. This implies that the water content in the lake and the ponds for example cannot be separated easily based on optical sensing. Worst NDWI results were obtained with ETM+/TM band 7.

5.2. Multiresolution analysis and automated lake extraction

We note that the five levels of segmentation (aggregation) present different feature information contents. For this case study the second and third levels were the optimal for the recognition and visualization of the lake. The approach ignores noise related to specific features at different scales. At 120 m resolution, the water–land boundary detection and visualization is demonstrated to be feasible. Even at the stage of texture extraction using wavelets, not only is the lake clearly isolated from the neighboring pixels, but also the shorelines are more well defined compared the resulting fuzzy cases of using NDWI. This preempts the fact that

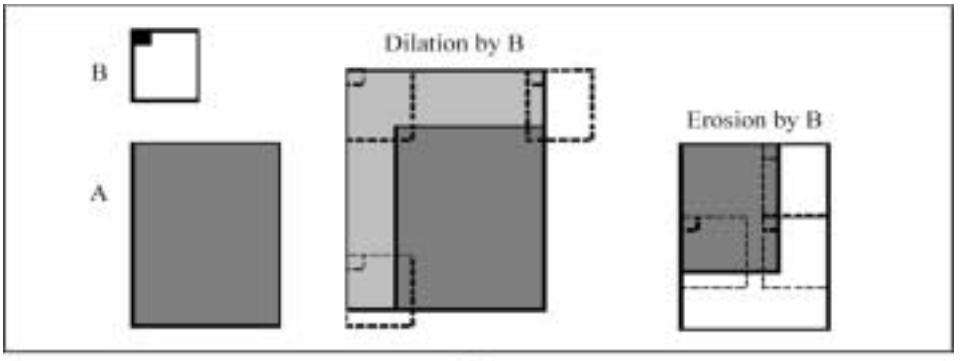

(a)

Data and Date	Enhanced and filtered image	Smoothened image
Landsat MSS (1976)		
Landsat TM (1986)		
Landsat ETM+ (2001)		
Scale	N	0 5 Km

(b)

Figure 13. (a) Dilation and erosion by kernel (B) on image A; (b) Landsat MSS (1976), Landsat TM (1986) and Landsat ETM+ (2001), respectively. Removing high frequency noise and preserving the boundaries of structures of interest, FOI, is the result of the diffusion process.

Figure 14. 1976 scanned map of Lake Nakuru-white tone. The map was derived from aerial photography, therefore reliable for analytical comparisons (not to scale).

controlling the spectral aggregation via the derived texture will automatically give better results than using spectral only information. The accuracy is further ensured by the automatic multiresolution analysis that gives a threshold of the suitable spatial resolution for FOI detection in the aggregation process.

It is evident from the results that spatially dominant features, e.g. lakes, tend to persist within one or two levels of scale domains and then suddenly disintegrate and new structures emerge. The trends observed in this study may be termed ‘creation’, ‘merging’ and ‘annihilation’ [24]. This approach renders itself suitable for mapping the dynamism of change through scale. The compensating advantages that this technique will provide are illustrated in comparison with conventional methods like NDWI in different spatial domains.

The accurate mapping of the lake’s extent and change is of paramount significance in GIS and spatial statistics analysis. In GIS applications, the boundary of connected components, e.g. the lakes, can be extracted into the vector module. Area computations and other lake related spatial analysis can then be made within a reference coordinate system. In hydrological resources management, determination of such parameters as wetland inundation (the temporal variation of water or hydroperiod) can adequately use the results of this research. The mass transfer coefficient ($K_E = 1.69*10^{-5}*A_L^{-0.05}$), computed from the surface area (A_L), is useful in the lake mass balance computation.

6. Conclusion

In this paper, we described an effective unsupervised-reproducible feature selection algorithm based on the association of textural and spectral characteristics of remotely sensed

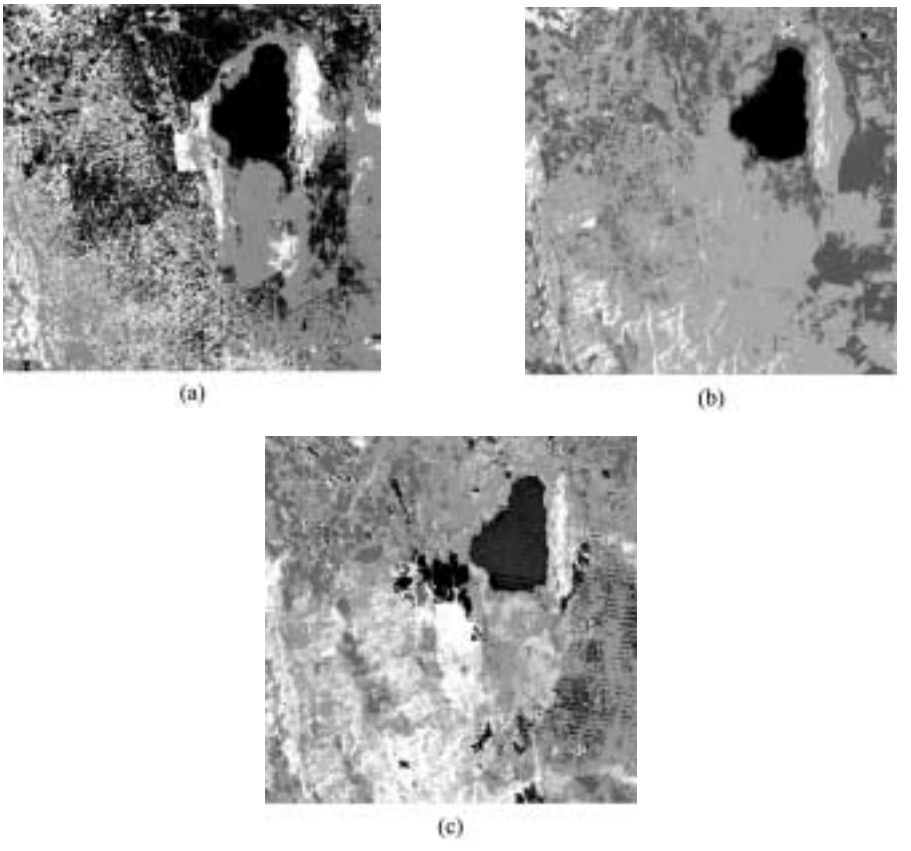

Figure 15. NDWI(=(Green-NIR)/(Green+NIR)) for: (a) ETM+, (b) TM and (c) MSS.

(RS) imagery, for extraction of water bodies (lake). Wavelet transformation has been used as a basis for the texture measures because of their characteristics of multiresolution and multi-direction in texture analysis, hence an improvement to the segmentation process. Anisotropic diffusion neural network method has been used in extracting the lake water through the texture based multilevel/multiscale segmentation. It has more advantages over the statistical based methods due to strong abilities of non-linear mapping and good self-adaptability. Both these methods combined the concept of scale-space for FOI detection.

The above results indicate that the Lake Nakuru shrank by about 18.8% between 1976 and 2001. This translates to averagely 0.6% per year (figure 17). The lake can shrink by up to 85% and bounce back to nearly its original size. Nevertheless, the lake is reducing in size, and the recent years, faster as seen in the gradients between (1976–1986) and (1986–2001) in figure 17. The main advantage of this method is that the computations can be performed in a lower-dimensional space that essentially preserves the discriminative information and provides features/bands that are approximately decorrelated. The main conclusions and recommendations that can be drawn from the present studies and from our experiments are as follows:

(1) Current standard techniques for analysis of remote sensing imagery mostly make use in spectral information only. These techniques normally neglect the neighborhood of the

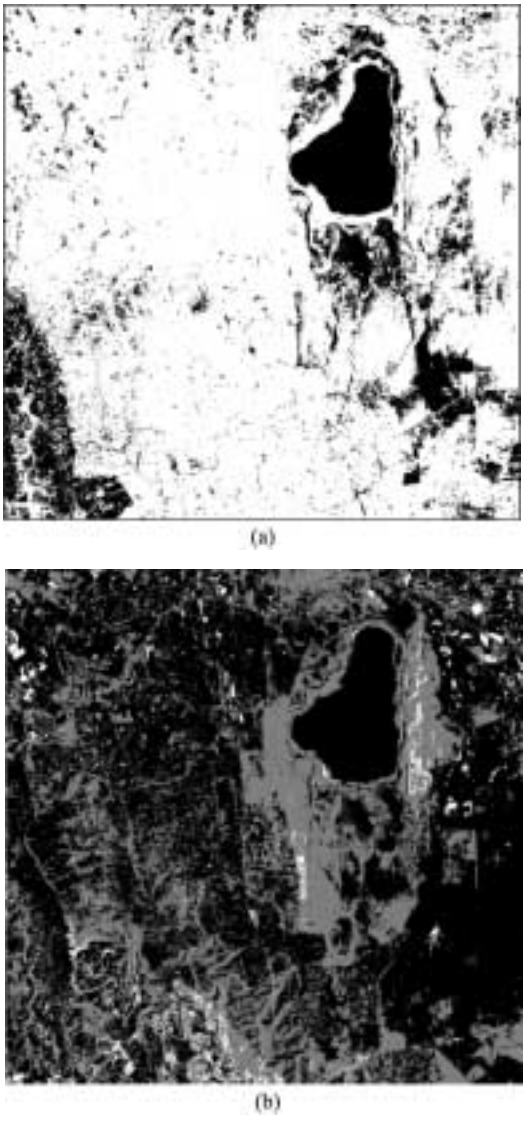

Figure 16. NDWI(=(NIR-SWIR)/(NIR+SWIR)) for: (a) ETM+ and (b) TM.

pixel(s) under investigation, which is the context information. Thus part of the data information is not used in the data analysis. This renders methods like ISODATA, NDWI, PCA, thresholding and even maximum-likelihood not robust in such sensitive analysis as this study. The scheme reported in this research has attempted to overcome this drawback.

(2) With the availability of just a few optical satellite sensors to choose from, which if anything have very similar spectral wavelengths especially in the NIR, better methods are desired for such tasks as lake water shoreline extraction.

(3) Through this approach, it is demonstrated that it is possible and simpler to compare multi-temporal data.

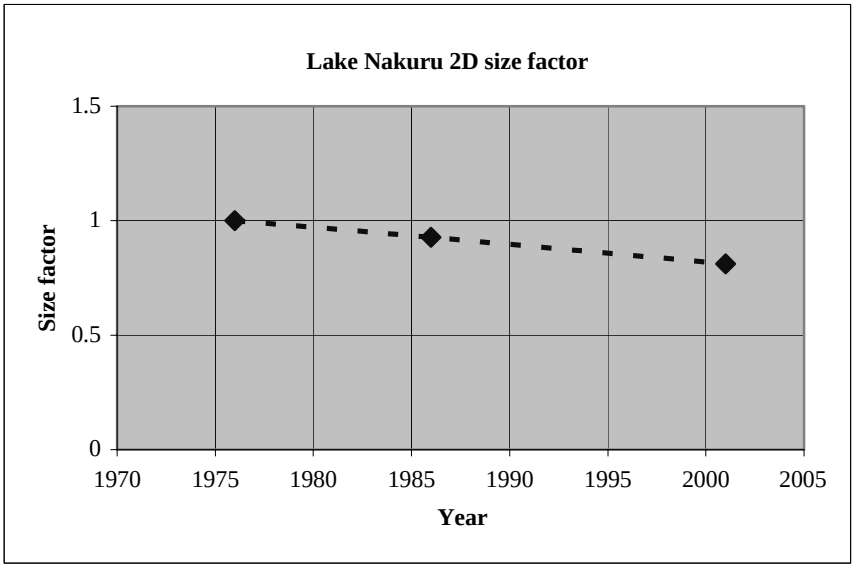

Figure 17. Three time series depicting fluctuation of Lake Nakuru. The line is dotted since in-between lake surface areas are highly variable and we have merely presented an average depicting reduction only.

(4) The multiscale aggregation process copes well with land-cover types with varying degrees of spectral complexity and spatial scale. Thus, is can delineate specific features of interest in complicated scenarios.

To quantify further the results rigorous ground observations need to be made. At this stage, out emphasis is in the testing of FOI detection. Research on validation techniques is under consideration.

References

[1] Braud, D.H. and Feng, W., 1998, Semi-automated construction of the Louisiana coastline digital land/water boundary using Landsat Thematic Mapper satellite imagery. Louisiana Applied Oil Spill Research and Development Program, OSRAPD Technical Report Series 97-002. Louisiana State University.

[2] Jupp, D.L.B., Mayo, K.K., Kuchler, D.A., Heggen, S.J. and Kendall, S.W., 1985, Landsat based interpretation of the cairns section of the great barrier reef marine park. *The CSIRO Natural Resources Series No. 4.*

[3] Moller-Jensen, L., 1990, Knowledge-based classification of an urban area using texture and context information in Landsat TM imagery. *Photogrammetric Engineering and Remote Sensing,* **56**(4), 475–479.

[4] McFeeters, S.K., 1996, The use of normalized difference water index (NDWI) in the delineation of open water features. *International Journal of Remote Sensing,* **7**(8), 1425–1432.

[5] Carvalho, M.T., Fonseca, L.M.G., Murtagh, F. and Clevers, J.G.P.W., 2001, Digital change detection with the aid of multiresolution analysis. *International Journal of Remote Sensing,* **22**(8), 3871–3876.

[6] Xiuwen, L., Chen, K. and Wang, D.L., 1999, Extraction of hydrographic regions from remote sensing images using an oscillator network with weight adaptation. Technical Report OSU-CISRC-4/99-TR12, The Ohio State University.

[7] Decatu, S.E., 1989, Application of neural networks to terrain classification. Paper presented at the IEEE Joint Conference on Neural Networks, pp. 283–288.

[8] Wilson, P.A., 1997, Rule-based classification of water in Landsat MSS images using the variance filter. *Photogrammetric Engineering and Remote Sensing,* **63**(5), 485–491.

[9] Marr, D. and Hildreth, E.C., 1980, Theory of edge detection. *Proceedings Royal Society of London,* **B-207,** 187–217.

[10] Franklin, J. and Woodcock, C., 1997, Multiscale vegetation data for the mountains of Southern California: spatial and categorical resolution. In: D.A. Quattrochi and M.F. Goodchild (Eds), *Scale in Remote Sensing and GIS* (Boca Raton, FL: Lewis Publishers), pp. 141–168.
[11] Bian, L., 1997, Multiscale nature of spatial data in scaling up environment models. In: D.A. Quattrochi and M.F. Goodchild (Eds), *Scale in Remote Sensing and GIS* (Boca Raton, FL: Lewis Publishers), pp. 13–27.
[12] DeFries, R.S., Townshend, J.R. and Los, S.O., 1997, Scaling land cover heterogeneity for global atmosphere-biosphere models. In: D.A. Quattrochi and M.F. Goodchild (Eds), *Scale in Remote Sensing and GIS* (Boca Raton, FL: Lewis Publishers), pp. 231–246.
[13] Turner, S.J., O'Neill, R.V., Conley, W. and Humphries, H.C., 1991, Pattern and scale: statistics for landscape ecology. In: M.G. Turner and R.H. Gardner (Eds), *Quantitative Methods in Landscape Ecology* (New York: Springer Verlag), pp. 17–50.
[14] Cao, C. and Lam, S.-N., 1997, Understanding the scale and resolution effects in remote sensing and GIS. In: D.A. Quattrochi and M.F. Goodchild (Eds), *Scale in Remote Sensing and GIS* (Boca Raton, FL: Lewis Publishers), pp. 57–72.
[15] Turner, M.G., Gardner, R.H. and O'Neill, R.U., 2001, *Landscape Ecology in Theory and Practice: Pattern and Process* (New York: Springer).
[16] Townshend, J.R.G. and Justice, C.O., 1988, Selecting the spatial resolution of satellite sensors required for global monitoring of land transformation. *International Journal of Remote Sensing*, **9,** 187–236.
[17] Mallat, S.G., 1989, A theory for multiresolution signal decomposition: the wavelet representation. *IEEE Transactions on Pattern Analysis and Machine Intelligence,* **12**(7), 629–639.
[18] Lark, R.M., 1996, Geostatistical description of texture on an aerial photograph for discriminating classes of land cover. *International Journal of Remote Sensing,* **17**(11), 2115–2133.
[19] Myint, S.W., 2001, A robust texture analysis and classification approach for urban land-use and land-cover feature discrimination. *Geocarto International,* **16**(4), 27–37.
[20] Ouma, Y.O. and Tateishi, R., 2004, A preliminary investigation into the application of wavelets transform as a fast-unsupervised environmental change detection strategy. Paper presented at the Indonesia–Japan Joint Scientific Symposium, Chiba University, Japan, 20–22 October.
[21] Perona, P. and Malik, J., 1987, Scale space and edge detection using anisotropic diffusion. Paper presented at the IEEE Computer Society Workshop on Computer Vision, Miami, Florida.
[22] Perona, P. and Malik, J., 1990, Scale-space and edge detection using anisotropic diffusion. *IEEE Transactions on Pattern Analysis and Machine Intelligence,* **12**(7), 629–639.
[23] Saint-Marc, P., Chen, J. and Medioni, G., 1991, Adaptive smoothing: a general tool for early vision. *IEEE Transactions on Pattern Analysis and Machine Intelligence,* **13**(6), 514–529.
[24] Hay, G.J., Marceau, D.J., Bouchard, A. and Dube, P., 2001, A multiscale framework for landscape analysis: object-specific up-scaling. *Landscape Ecology,* **16**, 471–490.